

# The correlation between C/O ratio, metallicity and the initial WD mass for SNe Ia

Xiangcun Meng<sup>1</sup> and Wuming Yang<sup>1,2</sup>

<sup>1</sup> School of Physics and Chemistry, Henan Polytechnic University, Jiaozuo, 454000, China  
e-mail: xiangcunmeng@hotmail.com

<sup>2</sup> Department of Astronomy, Beijing Normal University, Beijing 100875, China

Received; accepted

## ABSTRACT

**Context.** When type Ia supernovae (SNe Ia) were chosen as distance indicator to measure cosmological parameters, Phillips relation was applied. However, the origin of the scatter of the maximum luminosity of SNe Ia (or the variation of the production of <sup>56</sup>Ni) is still unclear. The metallicity and the carbon abundance of white dwarf (WD) before supernova explosion are possible key, but neither of them has an ability to interpret the scatter of the maximum luminosity of SNe Ia.

**Aims.** In this paper, we want to check whether or not the carbon abundance can be affected by initial metallicity.

**Methods.** We calculated a series of stellar evolution.

**Results.** We found that when  $Z \leq 0.02$ , the carbon abundance is almost independent of metallicity if it is plotted against the initial WD mass. However, when  $Z > 0.02$ , the carbon abundance is not only a function of the initial WD mass, but also metallicity, i.e. for a given initial WD mass, the higher the metallicity, the lower the carbon abundance. Based on some previous studies, i.e. both a high metallicity and a low carbon abundance lead to a lower production of <sup>56</sup>Ni formed during SN Ia explosion, the effects of the carbon abundance and the metallicity on the amount of <sup>56</sup>Ni are enhanced by each other, which may account for the variation of maximum luminosity of SNe Ia, at least qualitatively.

**Conclusions.** Considering that the central density of WD before supernova explosion may also play a role on the production of <sup>56</sup>Ni and the carbon abundance, the metallicity and the central density are all determined by the initial parameters of progenitor system, i.e. the initial WD mass, metallicity, orbital period and secondary mass, the amount of <sup>56</sup>Ni might be a function of the initial parameters. Then, our results might construct a bridge linking the progenitor model and the explosion model of SNe Ia.

**Key words.** Stars: white dwarfs - stars: supernova: general

## 1. Introduction

In their function as one of the distance indicators, type Ia supernovae (SNe Ia) show their importance in determining cosmological parameters, which resulted in the discovery of the accelerating expansion of the universe (Riess et al. 1998; Perlmutter et al. 1999). The result was exciting and suggested the presence of dark energy. At present, SNe Ia are proposed to be cosmological probes for testing the evolution of the dark energy equation of state with time and testing the evolutionary history of the universe (Riess et al. 2007; Kuznetsova et al. 2008; Howell et al. 2009a).

When SNe Ia are applied as a distance indicator, the Phillips relation is adopted, which is a linear relation between the absolute magnitude of SNe Ia at maximum light and the magnitude drop of the B light curve during the first 15 days following the maximum (Phillips 1993). This relation was motivated by the observations of two peculiar events, i.e. SN 1991bg and SN 1991T, and implies that the brightness of SNe Ia is mainly determined by one parameter. There is a consensus that a SN Ia is from a thermonuclear explosion of a carbon-oxygen white dwarf (CO WD) and the amount of <sup>56</sup>Ni formed during the supernova explosion dominates the maximum luminosity of SNe Ia (Arnett 1982). But the origin of the variation of the amount of <sup>56</sup>Ni for different SNe Ia is still unclear (Podsiadlowski et al. 2008). Many efforts have been paid to resolve this problem.

Some multi-dimensional numerical simulations showed that the ignition intensity (the number of ignition points) in the center of WDs or the transition density from deflagration to detonation are wonderful parameters interpreting the Phillips relation (Hillebrandt & Niemeyer 2000; Höflich et al. 2006, 2010; Kasen et al. 2010). In addition, the ratio of nuclear-statistical-equilibrium (NES) to intermediate-mass elements (IME) in the explosion ejecta is likely the key parameter for the width of SN Ia light curve and its peak luminosity (Pinto & Eastman 2001; Mazzali et al. 2001, 2007). For the simulations above, a reasonable assumption is that these parameters are determined by one or some properties of SNe Ia progenitor. Since these parameters are free ones for the numerical simulations of SNe Ia explosion, the question was turned into which property or properties of progenitor system determine these parameters. This is still unclear. Lesaffre et al. (2006) carried out a systematic study of the sensitivity of ignition conditions for H-rich Chandra single degenerate exploders on various properties of the progenitors, and suggested that the central density of the WD at ignition may be the origin of the Phillips relation (see also Podsiadlowski et al. 2008). This suggestion was upheld by detailed multi-dimensional numerical simulations of explosion (Krueger et al. 2010). But in the models of Höflich et al. (2010), the central density is only a second parameter, and the cooling time of the WDs before mass transfer in Lesaffre et al. (2006) and Krueger et al. (2010) is shorter than 1 Gyr. However, there are SNe Ia as old as 10 Gyr. The WDs with such a long cooling time may be-

come more degenerate before the onset of accretion phase. Some other processes like C and O separation or crystallization may occur, and dominate the properties of the CO WD (Fontaine et al. 2001). How the extremely degenerate conditions affect the properties of SNe Ia is still unclear. Then, the suggestion of Lesaffre et al. (2006) should be checked carefully under extremely degenerate conditions (Bravo et al. 2010b). Some numerical and synthetic studies showed that metallicity has an effect on the final amount of  $^{56}\text{Ni}$ , and thus the maximum luminosity (Timmes et al. 2003; Travaglio et al. 2005; Podsiadlowski et al. 2006; Bravo et al. 2010a) and there do be some observational evidence of the correlation between the properties of SNe Ia and metallicity (Branch & Bergh 1993; Hamuy et al. 1996; Wang et al. 1997; Cappellaro et al. 1997; Shanks et al. 2002). However, the metallicity seems not to have the ability to interpret the whole scatter of the maximum luminosity of SNe Ia (Timmes et al. 2003; Gallagher et al. 2008; Howell et al. 2009b).

Nomoto et al. (1999, 2003) suggested that the average<sup>1</sup> ratio of carbon to oxygen (C/O) of a white dwarf at the moment of explosion is the dominant parameter for the Phillips relation (see also Umeda et al. 1999b). The higher the C/O, the larger the amount of nickel-56, and then the higher the maximum luminosity of SNe Ia. By comparing theory and observations, the results of Meng, Chen & Han (2009) and Meng & Yang (2010a) upheld this suggestion. Nomoto et al. (1999, 2003) used total  $^{12}\text{C}$  mass fraction included in the convective core of mass  $M = 1.14M_{\odot}$  just before the SN Ia explosion,  $X(c)$ , to represent the C/O ratio and their suggestion is based on a fact that the dependence of  $X(c)$  on metallicity is small when it is plotted against the initial mass of WDs when  $Z \leq 0.02$ . Actually, when  $Z \leq 0.02$ , the effect of metallicity on the amount of  $^{56}\text{Ni}$  can be neglected. Only when  $Z > 0.02$ , metallicity has a significant influence on the production of  $^{56}\text{Ni}$  in SNe Ia explosion (Timmes et al. 2003). Here, we want to check whether or not the C/O ratio still can not be affected by metallicity when  $Z > 0.02$ .

In section 2, we simply describe our method, and present the calculation results in section 3. In section 4, we show discussions and our main conclusions.

## 2. METHOD

In this paper, our work is based on the single degenerate scenario, i.e. a SN Ia is from a CO WD in a binary system and its companion is a main-sequence or a slightly evolved star (WD+MS), a red giant star (WD+RG) or a helium star (WD + He star) (Whelan & Iben 1973; Nomoto, Thielemann & Yokoi 1984). This scenario has been widely studied by many groups (Li & van den Heuvel 1997; Hachisu et al. 1999a; Langer et al. 2000; Han & Podsiadlowski 2004; Chen & Li 2007; Hachisu et al. 2008; Meng, Chen & Han 2009; Lü et al. 2009; Wang et al. 2009a, 2009b; Meng & Yang 2010b, 2010c; Wang, Li & Han 2010). We assume that an initial CO WD is derived from a main sequence (MS) star in a primordial binary system (primary). The CO WD accretes hydrogen-rich material from its companion via Roche lobe overflow or wind, where the companion is a normal star. The accreted hydrogen-rich material is burned into helium, and then the helium is converted to carbon and oxygen. The CO WD increases its mass until the mass reaches  $1.378 M_{\odot}$  (close to the Chandrasekhar mass limit, Nomoto, Thielemann & Yokoi 1984) where it explodes in a thermonuclear supernova. A binary systems with the same primordial primary but different orbital

period may produce a CO WD with different mass. For simplicity, we assume that if the MS mass of the primary in a primordial binary system is same, the initial mass of the CO WD from the binary system is same and is equal to the core mass derived from the envelope-ejection model in Han, Podsiadlowski & Eggleton (1994) and Meng et al. (2008) (see below in details). Because the primary in a binary system may lose its hydrogen envelope due to the influence of secondary before it fulfills the criterion for the envelope ejection, the initial mass of CO WD in this paper should be taken as an upper limit for a real case. Actually, this assumption can not affect our results since we only want to find a relation between the C/O ratio, the WD mass and metallicity. The method used here is similar to that in Umeda et al. (1999a) and Höflich et al. (2010).

The C/O ratio before SN Ia explosion is a result of stellar and binary evolution, i.e. during central helium burning and thin shell burning during the stellar evolution and the accretion to close to the Chandrasekhar mass limit ( $1.378 M_{\odot}$ , Nomoto, Thielemann & Yokoi 1984). After the central helium burning phase, the C/O ratio is low, i.e. 0.25 – 0.5 depending on the initial mass and metallicity of main sequence (MS) star (Umeda et al. 1999a). The C/O ratio obtained from the burning shell is  $\approx 1$ , because the helium in the shell has a lower density and a higher temperature compared to helium burning in the core (Höflich et al. 2010).

In the paper, we calculate a series of stellar evolutions with the primordial MS mass from  $1 M_{\odot}$  to  $6.5 M_{\odot}$  until the stars evolve to the asymptotic giant branch (AGB) stage. When a star evolves to the stage, its envelope may be lost if the binding energy (BE) of the envelope transforms from a negative phase to positive one (Paczynski & Ziolkowski 1968, see also Fig. 2 in Meng et al. 2008). We calculated the BE of the envelope by

$$\Delta W = \int_{M_c}^{M_s} \left( -\frac{Gm}{r} + U \right) dm, \quad (1)$$

where  $M_c$  is the core mass,  $M_s$  is the surface value of the mass coordinate  $m$ .  $U$  is the internal energy of thermodynamics where those due to ionization of H and dissociation of  $\text{H}_2$ , as well as the basic  $\frac{3}{2} \mathcal{R}T/\mu$  for a perfect gas are all included). Here, we assume that a star will lose its envelope when the BE of the star's envelope increases to the point of  $\Delta W = 0$  and the core mass at the point is the final WD mass. The method here is robust and its virtue is significant because we need not consider the specific mechanism of mass loss since the mass loss rate is very uncertainty (see Meng et al. 2008 in details about this method). We assume that the remnant after envelope ejection is a CO WD if carbon and oxygen have not been ignited at the moment of envelope ejection. Following shell burning, we assume that the C/O ratio is 1<sup>2</sup> until  $M_{\text{WD}} = 1.378M_{\odot}$  as did in Umeda et al. (1999a) and Höflich et al. (2010).

We use the stellar evolution code of Eggleton (1971, 1972, 1973), which has been updated with the latest input physics over the last three decades (Han, Podsiadlowski & Eggleton 1994; Pols et al. 1995, 1998). The chemistry of a WD is mainly determined by the competition of two major nuclear reactions powering the He burning, i.e.  $3\alpha$  and  $^{12}\text{C}(\alpha, \gamma)^{16}\text{O}$ . As discussed by

<sup>2</sup> In fact, for the core chemical profile produced during the AGB phase, the steady increase of the carbon abundance in the region adjacent to the inner flat profile is synthesized by the shell in the early AGB, whereas the following abrupt peak is left by the thermally pulsing phase. The slope of the profile produced during the early AGB depends on both the initial mass and metallicity, and the C/O=1 is not always a good approximation. However, to compare with previous results, we still simply make a constant-ratio assumption.

<sup>1</sup> If there is no special statement, the C/O ratio in this paper is the average value over the whole WD structure just before the SN explosion.

Imbriani et al. (2001) and Prada Moroni & Straniero (2002), the final C/O after the central helium exhaustion not only depends on the rate of these two reactions, but also is significantly influenced by the efficiency of convective mixing operating at the central helium burning phase. We set the ratio of mixing length to local pressure scale height,  $\alpha = l/H_p$ , to 2.0, and set the convective overshooting parameter,  $\delta_{OV}$ , to 0.12 (Pols et al. 1997; Schröder et al. 1997), which roughly corresponds to an overshooting length of  $0.25H_p$ . The two parameters are adopted during the whole evolution of star. For the occurrence of convective instability near the He exhaustion in the central core, some breathing pulses are expected. (Castellani 1985, 1989). This phenomenon may also occur naturally in our code. The reaction rates are from Caughlan & Fowler (1988), except for the  $^{12}\text{C}(\alpha, \gamma)^{16}\text{O}$  reaction which is taken from Caughlan et al. (1985). The range of metallicity is from 0.0001 to 0.1, i.e. 0.0001, 0.0003, 0.001, 0.004, 0.01, 0.02, 0.03, 0.04, 0.05, 0.06, 0.08, 0.1. The opacity tables for these metallicities are compiled by Chen & Tout (2007) from Iglesias & Rogers (1996) and Alexander & Ferguson (1994). For a given  $Z$ , the initial hydrogen mass fraction is assumed by

$$X = 0.76 - 3.0Z, \quad (2)$$

(Pols et al. 1998), and then the helium mass fraction is  $Y = 1 - X - Z = 0.24 + 2Z$ . Based on the correlation between  $X$ ,  $Y$  and  $Z$  used here, Pols et al. (1998) accurately reproduced the color-magnitude diagrams (CMD) of some clusters.

In this paper, we skip thermal pulses by taking a longer time-step to reduce computing time, i.e. we study the average evolution of thermally pulsing AGB models. This treatment on the thermal pulses may lose some information about the structural change of the envelope due to thermal pulse. However, these treatment will not affect our final results because the situation of  $\Delta W = 0$  is fulfilled before the onset of thermal pulse and after the point a simple assumption of  $C/O = 1$  is adopted (see also in Meng et al. 2008).

### 3. Results

In this paper, we use total carbon abundance to represent the C/O ratio and a core mass to represent the initial WD mass as did in Umeda et al. (1999b). In figure 1, we show the abundances of several elements in mass fraction in the inner core of three representative models with different metallicity at the moment of envelope ejection. In the figure, the H burning shell is located around the mass coordinate of  $m = 0.9M_\odot$ , which means that the remnants from the models have a similar mass, i.e. the initial WD mass from the stars is similar. An interesting feature in the figure is that the carbon abundance and the flat part of the carbon abundance profile in the inner core decrease with metallicities (Umeda et al. 1999a; Dominguez et al. 2001). The carbon abundance is mainly derived from the result of the competition between  $3\alpha$  and  $^{12}\text{C}(\alpha, \gamma)^{16}\text{O}$  reaction in the central helium burning phase, while the flat profile is the result of the central helium burning, which occurs in a convective core. An increase of the metallicity leads to an increase of the radiative opacity, and consequently, a decrease of the central temperature at given phase, the decrease of the He core mass at the  $3\alpha$  onset. For the central helium burning phase, this leads to a smaller convective core, hence a smaller region characterized by a flat C/O profile. A low central temperature favors the destruction reaction of  $^{12}\text{C}$ , namely the  $^{12}\text{C}(\alpha, \gamma)^{16}\text{O}$  with respect the  $3\alpha$  reaction, which is the main cause for the decrease of the central carbon abundance. In addition, the central carbon abundance is also relevant to the

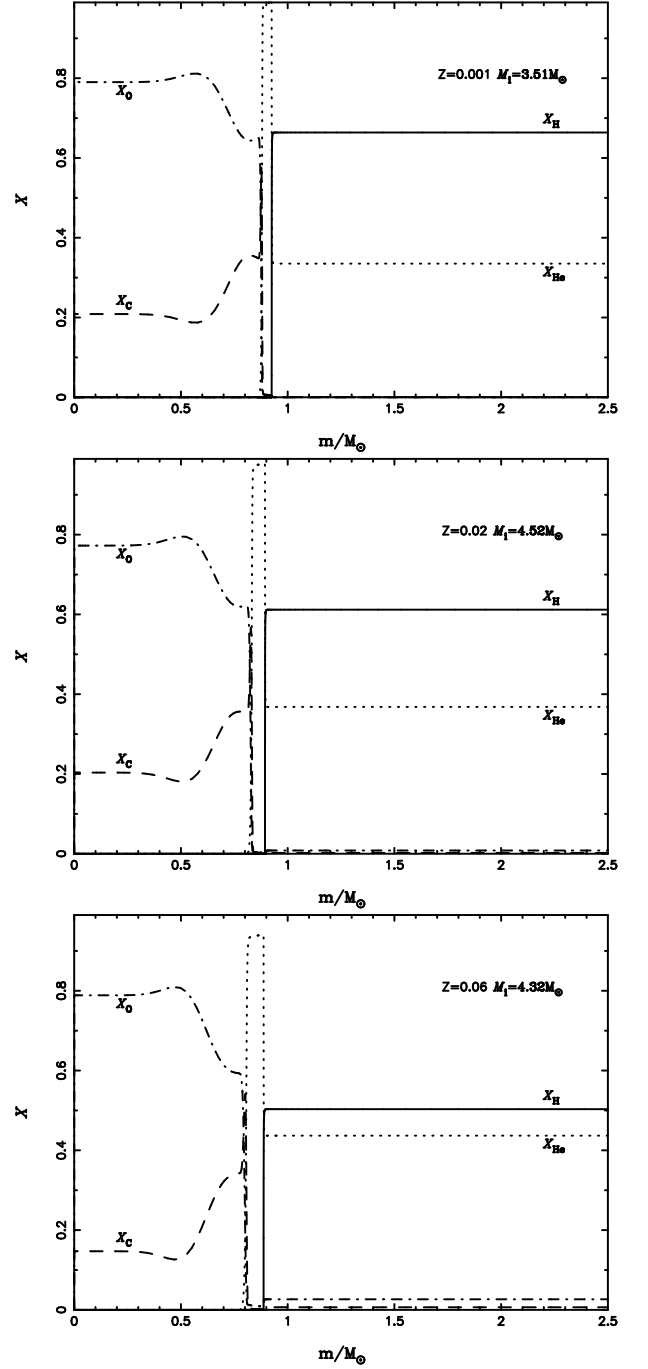


**Fig. 1.** Abundances of several elements in mass fraction in the inner core of three models with different primordial MS masses and different metallicities at the moment of envelope ejection. The solid, dotted, dashed and dot-dashed lines represent hydrogen, helium, carbon and oxygen abundance, respectively. Top:  $Z = 0.001$  and  $M_i = 3.51$ ; Middle:  $Z = 0.02$  and  $M_i = 4.52$ ; Bottom:  $Z = 0.06$  and  $M_i = 4.32$ .

helium abundance in central helium burning phase, and then to metallicity via  $Y = 1 - Z$  at the beginning of central helium burning. For a given temperature, a low helium abundance, i.e. a high metallicity, means a slight lower burning rates of  $3\alpha$  reaction. However, between the model of  $Z = 0.001$  and  $Z = 0.02$  in figure 1, the difference of carbon abundance is not significant, but the difference between the model of  $Z = 0.02$  and  $Z = 0.06$  is remarkable. Then, the effect of metallicity on the C/O ratio may

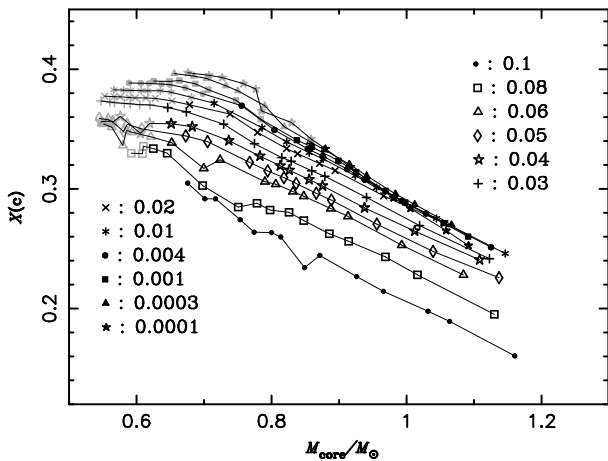


**Fig. 2.** The relation between the total carbon abundance of WDs before supernova explosion and the initial WD mass for SNe Ia with different metallicities. The gray points represent those that may not contribute to SNe Ia.

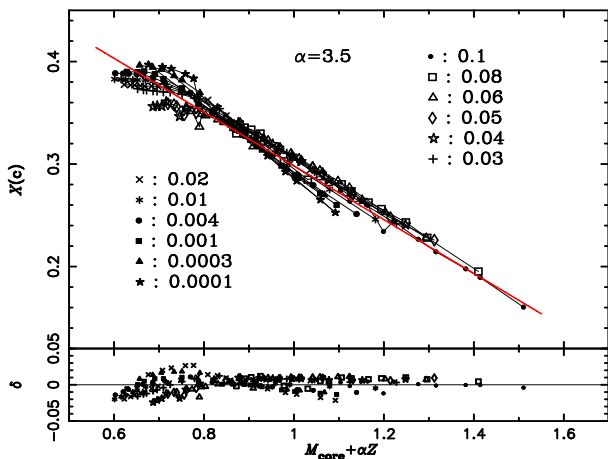


**Fig. 3.** The relation between the total carbon abundance of WDs before supernova explosion, the initial WD mass and metallicity. The solid line is the best fitted linear relation, where the line fits all the points shown in Fig. 2. The lower panel shows the difference between the points and the fitted line.

not be neglected when  $Z > 0.02$ . In addition, the hydrogen abundance decreases and helium abundance increase with metallicity in the figure, which is a natural result of equation 2<sup>3</sup>.

In figure 2<sup>4</sup>, we show the relation between the total carbon mass fraction of WDs before SNe Ia explosion and the initial WD mass for SNe Ia with different metallicities. For the cases of  $Z \leq 0.02$ , the results here is similar to that in Nomoto et al. (1999, 2003), i.e. the relation between the carbon abundance and the initial WD mass is independent of metallicity, especially for  $M_{\text{WD}} \geq 0.8M_{\odot}$ . When  $M_{\text{WD}} \leq 0.8M_{\odot}$ , the scatter is enlarged for the cases of  $Z \leq 0.02$ , which is mainly from low-

<sup>3</sup> The hydrogen abundance and the helium abundance are not accurately equal to those derived from equation 2 because of the first and second dredge-up (Busso et al. 1999).

<sup>4</sup> Here, the gray points are plotted based on the study in Meng et al (2009). Please keep in mind that the results for the lower limit of WDs for SNe Ia in Meng et al. (2009) may be higher than that in Meng & Yang (2010a) since some special effects such as mass-stripping effect of an optically thick wind and the effect of thermal unstable disk are considered in Meng & Yang (2010a).

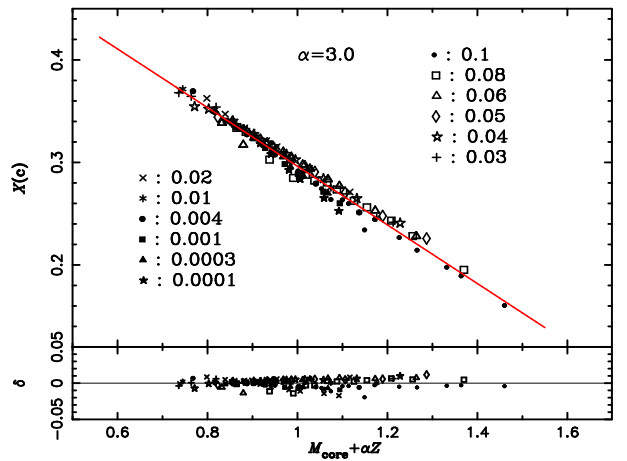


**Fig. 4.** The relation between the total carbon abundance of WDs before SNe Ia explosion, the initial WD mass and metallicity, where the points which may not contribute to SNe Ia are cut off. The solid line is the best fitted linear relation. The lower panel shows the difference between the points and the fitted line.

metallicity cases ( $\leq 0.001$ , see also Fig. 12 in Umeda et al. 1999a). However, for the low-metallicity cases, the WDs with a mass smaller than  $0.8M_{\odot}$  may not contribute to SNe Ia (see figure 5 in Meng, Chen & Han 2009).

A remarkable feature in figure 2 is that when  $Z > 0.02$ , the relation between the carbon abundance and the initial WD mass significantly deviates from those of  $Z \leq 0.02$  and the deviation increases with metallicity, i.e. for a given initial WD mass, a high metallicity leads to a lower carbon abundance as shown in figure 1. This is similar to that found by Timmes et al. (2003), i.e. only when  $Z > 0.02$ , the influence of metallicity becomes significant. So, the discovery of Umeda et al. (1999b) and Nomoto et al. (1999, 2003) is a low-metallicity limit of the result found in this paper.

In the three-dimensional space of  $(X_C, M_{\text{core}}, Z)$ , the relations between the carbon abundance and the initial WD mass with different metallicity are almost in a plane. We take the  $X_C$  as a function of  $M_{\text{core}} + \alpha Z$  and use the minimum  $\chi^2$  method to find the best relation. We found that a linear relation may well represent the relation when  $\alpha = 3.5$ . The best fitted relation is

$$X_C = 0.5531 - 0.2528(M_{\text{core}} + \alpha Z), \quad (3)$$

where  $\chi_{\text{min}}^2 = 5.16 \times 10^{-2}$ . We also try to use a parabola to fit the relation between  $X_C$  and  $M_{\text{core}} + \alpha Z$ , but the improvement is slight, i.e.  $\chi_{\text{min}}^2 = 4.84 \times 10^{-2}$ . Seen from the equation 3, both a high initial WD mass and a high initial metallicity lead to a lower carbon abundance. In addition, if the metallicity is low enough, its effect on the carbon abundance can be neglected. But the effect of a high metallicity is significant. For example, for a typical value of  $M_i = 0.8M_{\odot}$  (Meng, Chen & Han 2009; Meng & Yang 2010a), the uncertainty of  $X_C$  derived from metallicity for  $Z \leq 0.02$  is less than 5%, but may be as large as 25% for  $Z > 0.02$ .

If the points which may not contribute to SNe Ia in Fig. 2 are cut off, we even may obtain a more tight linear relation, i.e.  $X_C = 0.5824 - 0.2862(M_{\text{core}} + \alpha Z)$  where  $\alpha = 3.0$  and  $\chi_{\text{min}}^2 = 1.46 \times 10^{-2}$  (see Fig. 4).

#### 4. Discussions and conclusions

When one simulates the SN Ia explosion, the carbon abundance (the C/O ratio) and metallicity are always taken as free parameters. But neither of them has an ability to interpret the variation in the mass of  $^{56}\text{Ni}$  ejected by SNe Ia, especially for subluminous SNe Ia (such as 1991bg-like supernovae, Timmes et al. 2003; Röpke et al. 2006a; Bravo et al. 2010b). However, many evidence shows the correlation between the maximum luminosity of SNe Ia and metallicity. For example, many groups noticed that subluminous SNe Ia occur exclusive in massive galaxies (Neill et al. 2009; Sullivan et al. 2010; González-Gaitán et al. 2010; Lampeitl et al. 2010). Considering the mass-metallicity relation of galaxies (Tremonti et al. 2004), subluminous SNe Ia favor more metal-rich environments. In addition, some 1991T-like SNe Ia were discovered in metal-poor environments<sup>5</sup> (Prieto et al. 2008; Badenes et al. 2009; Khan et al. 2010). So, metallicity should play a more significant role in a rather wide range than that suggested in theory. The confliction between theory and observations should be resolved.

In this paper, we found that when  $Z > 0.02$ , the carbon abundance before SN Ia explosion is affected by not only initial WD mass but also metallicity. For a given initial WD mass, the higher the metallicity, the lower the carbon abundance. The relation between the carbon abundance, the initial WD mass and the metallicity may be represented by a simple linear relation. Thus, when one simulates the SN Ia explosion, the carbon abundance (the C/O ratio) and metallicity would not be taken as free parameters. Their effect on the amount of  $^{56}\text{Ni}$  is enhanced by each other since the effect of a high metallicity and a low carbon abundance on the amount of  $^{56}\text{Ni}$  is similar, i.e. producing a lower amount of  $^{56}\text{Ni}$  (Nomoto et al. 1999, 2003; Timmes et al. 2003). So, our result may account for the variation of the maximum luminosity of SNe Ia, at least qualitatively providing a method to conquer the confliction stated above. However, please keep in mind that whether or not the combined action of the C/O ratio and metallicity has enough ability to interpret the variation of the maximum luminosity of SNe Ia still should be verified carefully. So, we encourage someone to do a detailed numerical simulation on this problem based on the result here.

Furthermore, the central density at the moment of supernova explosion may also play a role to some extent (Höflich et al. 2010; Krueger et al 2010), and the carbon abundance, metallicity and the central density all contribute to the variation of the maximum luminosity of SNe Ia (Röpke et al. 2006b). By a simple assumption that the carbon abundance is the function of initial WD mass and the central density is determined by initial WD mass and its cooling time, Meng et al. (2010) noticed that the WDs with a high carbon abundance usually have a lower central density at ignition, while those having the highest central density at ignition generally have a lower carbon abundance. Interestingly, the effect of a high metallicity, a low C/O ratio and a high central density on the amount of  $^{56}\text{Ni}$  is similar, i.e. producing a less amount of  $^{56}\text{Ni}$  and thus a dimmer event (Nomoto et al. 1999, 2003; Timmes et al. 2003; Krueger et al 2010), then all of them could contribute the fact that elliptical galaxies favor the dim SNe Ia (Hamuy 1996). Although it is still unclear how the metallicity affects the central density, we may hypothesize optimistically that it is unreasonable that take the carbon

abundance, metallicity and the central density as free parameters when one simulates SN Ia explosion, and these parameters may all contribute the production of  $^{56}\text{Ni}$  (Röpke et al. 2006b), which could be a key to open the origin of the Phillips relation. Moreover, these parameters can be determined by the initial parameters of a progenitor system, i.e. the WD mass, metallicity, orbital period and secondary mass. For example, the C/O ratio is a function of the initial WD mass and metallicity, while the central density of a WD before supernova explosion is determined by accretion rate and its cooling time before the onset of mass transfer, which is related with the initial WD mass, secondary mass and period. Then our study might provide a bridge linking the progenitor model and explosion model of SNe Ia.

*Acknowledgements.* This work was partly supported by Natural Science Foundation of China under grant no. 11003003 and the Project of the Fundamental and Frontier Research of Henan Province under grant no. 102300410223, the Project of Science and Technology from the Ministry of Education (211102) and the China Postdoctoral Science Foundation funded project 20100480222.

#### References

- Alexander D. R., Ferguson J. W., 1994, ApJ, 437, 879  
 Arnett W.D., 1982, ApJ, 253, 785  
 Badenes C., Harris J., Zaritsky D. et al., 2009, ApJ, 700, 727  
 Branch D., Bergh S.V., 1993, AJ, 105, 2231  
 Bravo E., Domínguez I., Badenes C. et al., 2010a, ApJ, 711, L66  
 Bravo E., Althaus L.G., García-Berro et al. 2010b, A&A, in press, arXiv: 1010.5098  
 Busso M., Gallino R., & Wasserburg G. J. 1999, ARA&A, 37, 239  
 Cappellaro E., Turatto M., Tsvetkov D.Y. et al., 1997, A&A, 322,431  
 Castellani V., Chieffi A., Tornambe A., Pulone L., 1985, ApJ, 296, 204  
 Castellani V., Chieffi A., Pulone L., 1989, ApJ, 344, 239  
 Caughlan G.R., Fowler W.A., Harris M.J., Zimmerman B.A., 1985, At. Data Nucl. Data Tables, 35, 198  
 Caughlan G.R. & Fowler W.A., 1988, At. Data Nucl. Data Tables, 40, 284  
 Chen X., Tout C.A., 2007, ChJAA, 7, 2, 245  
 Chen W., Li X., 2007, ApJ, 658, L51  
 Domínguez I., Höflich P., Straniero O., 2001, ApJ, 557, 279  
 Eggelton P.P., 1971, MNRAS, 151, 351  
 Eggelton P.P., 1972, MNRAS, 156, 361  
 Eggelton P.P., 1973, MNRAS, 163, 279  
 Fontaine G., Brassard P., Bergeron P., 2001, PASP, 113, 409  
 Gallagher, J. S., Garnavich, P. M., Caldwell, N., Kirshner, R. P., Jha, S. W., Li, W., Ganeshalingam, M., Filippenko, A. V., 2008, ApJ, 685, 752  
 González-Gaitán S., Perrett K., Sullivan M. et al., 2010, arXiv: 1011.4531  
 Hachisu I., Kato M., Nomoto K. et al., 1999, ApJ, 519, 314  
 Hachisu, I., Kato, M., Nomoto, K., 2008, ApJ, 679, 1390  
 Hamuy M., Phillips M.M., Schommer R.A., et al., 1996, AJ, 112, 2391  
 Han Z., Podsiadlowski P., Eggelton P.P., 1994, MNRAS, 270, 121  
 Han Z., Podsiadlowski Ph., 2004, MNRAS, 350, 1301  
 Hillebrandt W., Niemeyer J.C., 2000, ARA&A, 38, 191  
 Höflich, P., Gerardy, C. L., Marion, H., & Quimby, R. 2006, NewAR, 50, 470  
 Höflich P., Krisciunas K., Khokhlov A.M. et al., 2010, ApJ, 710, 444  
 Howell D.A. et al., 2006, Nature, 443, 308  
 Howell, D.A. et al., 2009a, arXiv: 0903.1086  
 Howell, D.A. et al., 2009b, ApJ, 691, 661  
 Iglesias C. A., Rogers F. J., 1996, ApJ, 464, 943  
 Imbriani G., Limongi M., Gialanella L. et al. 2001, ApJ, 558, 903  
 Kasen, D., Röpke, F. K., Woosley, S.E., 2010, Nature, 460, 869  
 Khan R., Stanek K.Z., Prieto J.L. et al., 2010, ApJ, in press, arXiv:1008.4126  
 Krueger, B. K.; Jackson, A. P.; Townsley, D. M. et al., 2010, ApJ, 719, L5  
 Kuznetsova N., Barbary K., Connolly B. et al., 2008, ApJ, 673, 981  
 Lampeitl H., Smith M., Nichol R.C. et al., 2010, ApJ, 722, 565  
 Langer N., Deutschmann A., Wellstein S. et al., 2000, A&A, 362, 1046  
 Lesaffre P., Han Z., Tout C.A. et al., 2006, MNRAS, 368, 187  
 Li X.D., van den Heuvel E.P.J., 1997, A&A, 322, L9  
 Lü, G., Zhu, C., Wang, Z., Wang, N., 2009, MNRAS, 396, 1086  
 Mazzali P.A., Nomoto K., Cappellaro E., Nakamura T., Umeda H., Iwamoto K., 2001, ApJ, 547, 988  
 Mazzali P.A., Röpke F.K., Benetti S., Hillebrandt W., 2007, Science, 315, 825  
 Meng X., Chen X., Han Z., 2008, A&A, 487, 625  
 Meng X., Chen X., Han Z., 2009, MNRAS, 395, 2103

<sup>5</sup> Even 2003fg-like SNe Ia which are over-luminous events favor metal-poor environments (Taubenberger et al. 2010), but the discussion about these SNe Ia is beyond the scope of this paper since these SNe Ia are over Chandrasekhar mass limit (Howell et al. 2006) and this paper is based on the Chandrasekhar mass model.

- Meng X., Yang W., 2010a, *ApJ*, 710, 1310  
 Meng X., Yang W., 2010b, *A&A*, 516, A47  
 Meng X., & Yang W., 2010c, *MNRAS*, 401, 1118  
 Meng X., Yang W., Li Z., 2010, *RAA*, 10, 927  
 Neill J. D., Sullivan M., Howell D. A. et al. 2009, *ApJ*, 707, 1449  
 Nomoto K., Thielemann F.-K., Yokoi K., 1984, *ApJ*, 286, 644  
 Nomoto K., Umeda H., Hachisu I. et al., 1999, in Truran J., Niemeyer T., eds, *Type Ia Supernova : Theory and Cosmology*. Cambridge Univ. Press, New York, p.63  
 Nomoto K., Uenishi T., Kobayashi C. et al., 2003, in Hillebrandt W., Leibundgut B., eds, *From Twilight to Highlight: The Physics of supernova*, ESO/Springer serious "ESO Astrophysics Symposia" Berlin: Springer, p.115  
 Paczyński B., Ziółkowski L., 1968, *Acta Astron.*, 18, 225  
 Perlmutter S., Aldering G., Goldhaber G. et al., 1999, *ApJ*, 517, 565  
 Phillips M.M., 1993, *ApJ*, 413, L105  
 Pinto P.A., Eastman R.G., 2001, *NewA*, 6, 307  
 Podsiadlowski P., Mazzali P.A., Lesaffre P. et al., 2006, *astro-ph/0608324*  
 Podsiadlowski P., Mazzali P., Lesaffre P., Han, Z., Förster F., 2008, *NewAR*, 52, 381  
 Pols O.R., Tout C.A., Eggleton P.P. et al., 1995, *MNRAS*, 274, 964  
 Pols O.R., Tout C.A., Schröder K.P. et al., 1997, *MNRAS*, 289, 869  
 Pols O.R., Schröder K.P., Hurly J.R. et al., 1998, *MNRAS*, 298, 525  
 Prada Moroni P. & Straniero O., 2002, *ApJ*, 581, 585  
 Prieto J.L. et al., 2008, *ApJ*, 673, 999  
 Riess A.G., Filippenko A.V., Challis P. et al., 1998, *AJ*, 116, 1009  
 Riess A. et al., 2007, *ApJ*, 659, 98  
 Röpke F.K., Gieseler M., Reinecke M. et al., 2006a, *A&A*, 453, 203  
 Röpke F.K., Gieseler M., Hillebrandt W., 2006b, *arXiv:0609459*  
 Schröder K.P., Pols O.R., Eggleton P.P., 1997, *MNRAS*, 285, 696  
 Shanks T., Allen P.D., Hoyle F. et al., 2002, *ASPC*, 283, 274  
 Sullivan M., Conley A., Howell D. A. et al., 2010, *MNRAS*, 406, 782  
 Taubenberger S., Benetti S., Childress M. et al., 2010, *MNRAS*, in press, *arXiv:1011.5665*  
 Timmes F.X., Brown E.F., Truran J.W., 2003, *ApJ*, 590, L83  
 Travaglio C., Hillebrandt W., Reinecke M., 2005, *A&A*, 443, 1007  
 Tremonti C.A., Heckman T.M., Kauffmann G. et al., 2004, *ApJ*, 613, 898  
 Umeda H., Nomoto K., Yamaoka H., et al., 1999a, *ApJ*, 513, 861  
 Umeda H., Nomoto K., Kobayashi C. et al., 1999b, *ApJ*, 522, L43  
 Wang L., Höflich P., Wheeler J.C., 1997, *ApJ*, 483, L29  
 Wang, B., Meng, X., Chen, X., Han, Z., 2009a, *MNRAS*, 395, 847  
 Wang, B., Chen, X., Meng, X., Han, Z., 2009b, *ApJ*, 701, 1540  
 Wang B., Li X., Han Z., 2010, *MNRAS*, 401, 2729  
 Whelan J. & Iben I., 1973, *ApJ*, 186, 1007

## Appendix A: Some physical quantities for models

In this paper, we calculated a large and fine grid models. Here, we provide some physical quantities of the models such as CO core mass, total carbon abundance  $X(C)$ , initial main-sequence mass and metallicity, which may be helpful for completing the resolution in the field. Here, the boundary of the CO core was located at the 10% of the maximum helium abundance in the helium shell (see the left dotted line in Fig. 1).

**Table A.1.** The CO core masses (in  $M_{\odot}$ ) for different metallicities (in  $Z_{\odot}$ , Row 1) and different initial masses (Column 1, in  $M_{\odot}$ ). The bars represent models whose final fates are ONeMg white dwarfs.

	0.005	0.015	0.05	0.2	0.5	1.0	1.5	2.0	2.5	3.0	4.0	5.0
1.00	0.6683	0.6490	0.6196	0.5786	0.5531	0.5366	0.5283	0.5272	0.5240	0.5292	0.5698	0.6358
1.30	0.7033	0.6798	0.6433	0.5981	0.5698	0.5533	0.5438	0.5406	0.5403	0.5435	0.5844	0.6438
1.50	0.7266	0.7007	0.6602	0.6112	0.5812	0.5634	0.5538	0.5503	0.5477	0.5609	0.5877	0.6450
1.80	0.7562	0.7281	0.6846	0.6308	0.5985	0.5784	0.5687	0.5621	0.5659	0.5687	0.6036	0.6481
2.00	0.7746	0.7488	0.7038	0.6437	0.6094	0.5881	0.5788	0.5749	0.5724	0.5774	0.6242	0.6698
2.29	0.7725	0.7863	0.7454	0.6680	0.6284	0.6051	0.5953	0.5938	0.5943	0.6060	0.6698	0.6736
2.51	0.8258	0.7898	0.7637	0.6939	0.6449	0.6196	0.6109	0.6093	0.6223	0.6378	0.6764	0.6973
2.79	0.8319	0.8208	0.7961	0.7515	0.6761	0.6460	0.6373	0.6410	0.6648	0.6747	0.6856	0.7737
2.99	0.8522	0.8420	0.8178	0.7640	0.7093	0.6718	0.6657	0.6729	0.6872	0.6894	0.7027	0.7777
3.31	0.8884	0.8804	0.8570	0.7971	0.7921	0.7323	0.7120	0.7120	0.7115	0.7136	0.7377	0.7913
3.51	0.9112	0.9059	0.8837	0.8187	0.7674	0.7411	0.7308	0.7292	0.7276	0.7289	0.7573	0.8208
3.80	0.9500	0.9461	0.9258	0.8563	0.7978	0.7647	0.7550	0.7512	0.7526	0.7564	0.7899	0.8765
3.98	0.9748	0.9740	0.9543	0.8801	0.8176	0.7805	0.7699	0.7652	0.7711	0.7761	0.8145	0.9095
4.32	1.0252	1.0274	1.0159	0.9313	0.8620	0.8134	0.7983	0.7977	0.7992	0.8124	0.8619	0.9869
4.52	1.0561	–	1.0669	0.9661	0.8898	0.8367	0.8166	0.8167	0.8199	0.8351	0.8971	–
5.01	–	–	–	1.0816	0.9733	0.9013	0.8725	0.8727	0.8833	0.9049	0.9983	–
5.50	–	–	–	–	1.0913	0.9869	0.9391	0.9431	0.9582	0.9956	–	–
6.03	–	–	–	–	–	–	1.0448	1.0476	1.0710	–	–	–

**Table A.2.** The total carbon mass fraction of WDs before SNe Ia explosion for different metallicities (in  $Z_{\odot}$ , Row 1) and different initial masses (Column 1, in  $M_{\odot}$ ). The bars represent models whose final fates are ONeMg white dwarfs.

	0.005	0.015	0.05	0.2	0.5	1.0	1.5	2.0	2.5	3.0	4.0	5.0
1.00	0.3971	0.3964	0.3901	0.3886	0.3828	0.3775	0.3735	0.3560	0.3589	0.3543	0.3298	0.3048
1.30	0.3949	0.3943	0.3898	0.3883	0.3825	0.3771	0.3726	0.3566	0.3578	0.3516	0.3294	0.2917
1.50	0.3930	0.3923	0.3906	0.3881	0.3823	0.3770	0.3721	0.3563	0.3561	0.3364	0.3357	0.2917
1.80	0.3879	0.3861	0.3878	0.3876	0.3821	0.3764	0.3714	0.3607	0.3480	0.3489	0.3337	0.2743
2.00	0.3835	0.3820	0.3829	0.3871	0.3820	0.3761	0.3711	0.3550	0.3540	0.3474	0.3298	0.2638
2.29	0.3653	0.3696	0.3741	0.3845	0.3821	0.3760	0.3704	0.3464	0.3501	0.3435	0.3028	0.2635
2.51	0.3554	0.3520	0.3582	0.3795	0.3808	0.3757	0.3702	0.3547	0.3478	0.3386	0.2848	0.2598
2.79	0.3417	0.3395	0.3408	0.3695	0.3765	0.3735	0.3680	0.3544	0.3443	0.3172	0.2880	0.2342
2.99	0.3335	0.3327	0.3350	0.3493	0.3716	0.3702	0.3645	0.3520	0.3395	0.3243	0.2823	0.2444
3.31	0.3184	0.3207	0.3235	0.3334	0.3512	0.3625	0.3541	0.3403	0.3221	0.3060	0.2804	0.2267
3.51	0.3080	0.3110	0.3140	0.3275	0.3393	0.3472	0.3378	0.3274	0.3150	0.3040	0.2735	0.2144
3.80	0.2925	0.2958	0.2984	0.3165	0.3303	0.3337	0.3262	0.3193	0.3094	0.2978	0.2625	0.1977
3.98	0.2836	0.2870	0.2886	0.3078	0.3250	0.3294	0.3231	0.3156	0.3045	0.2939	0.2562	0.1893
4.32	0.2651	0.2700	0.2714	0.2899	0.3111	0.3212	0.3151	0.3078	0.2964	0.2836	0.2432	0.1605
4.52	0.2526	–	0.2601	0.2794	0.3009	0.3153	0.3105	0.3026	0.2907	0.2770	0.2282	–
5.01	–	–	–	0.2512	0.2753	0.2942	0.2928	0.2842	0.2706	0.2530	0.1952	–
5.50	–	–	–	–	0.2460	0.2712	0.2693	0.2647	0.2477	0.2281	–	–
6.03	–	–	–	–	–	–	0.2416	0.2407	0.2258	–	–	–